Coupling Laplace Transform with Residual Power Series: A Novel Route to Enhance Nonlinear Time-Fractional Whitham–Broer–Kaup Models

FARES BEKHOUCHE[1] , IQBAL M. BATIHA[2,3,*], OUIDAD BOULAKOUR[4],
RADWAN M. BATYHA[5], AHMED BOUCHENAK[6,7], SHAHER MOMANI[3,8]

[1]Laboratory of Mathematics and Artificial Intelligence,
Department of Mathematics,
Abbes Laghrour University,
Khenchela 40000, ALGERIA

[2]Department of Mathematics,
Al Zaytoonah University of JORDAN,
Amman, 11733, JORDAN

[3]Nonlinear Dynamics Research Center (NDRC),
Ajman University,
Ajman, 346, UAE

[4] Laboratory of Dynamical Systems and Control,
Department of Mathematics and Computer Science,
University of Oum El Bouaghi,
Oum El Bouaghi 04000,
ALGERIA

[5] Department of Computer Science
Applied Science Private University
Amman 11931, JORDAN

[6]Department of Mathematics,
University Mustapha Stambouli of Mascara,
Mascara, 29000, ALGERIA

[7]Laboratory of Applied Mathematics and Modeling,
Université 8 Mai 1945,
B.P. 401, Guelma, 24000, ALGERIA

[8]Department of Mathematics,
University of Jordan,
Amman, JORDAN

Abstract: Due to the limitations of the Laplace transform in solving certain classes of nonlinear partial differential equations, this study introduces a novel numerical technique that combines the Laplace transform with the residual power series approach to effectively handle the nonlinear time-fractional Whitham–Broer–Kaup (WBK) equations. The newly developed method, called the Laplace-Residual Power Series Method (L-RPSM), integrates the strengths of both techniques to overcome the restrictions encountered when each method is applied individually.
In this approach, the fractional derivative is defined in the sense of the Caputo derivative. To demonstrate the applicability and efficiency of the proposed method, the nonlinear time-fractional WBK equations are solved step by step, and the obtained approximate solutions are analyzed in detail. The performance of the L-RPSM is validated through a numerical application, where the results are presented in tables, two-dimensional plots, and three-dimensional graphs.
The results show that the L-RPSM is not only robust and efficient but also straightforward to implement. It provides rapidly convergent series solutions with very high accuracy, confirming its capability to approximate the exact solutions of the WBK equations. In addition, the flexibility of the method allows its application to various fractional partial differential equations, confirming its role as a reliable and versatile approach for analyzing nonlinear fractional systems.

Key-Words: Caputo fractional derivative, Laplace transform, Laplace-residual power series method, the nonlinear time-fractional Whitham–Broer–Kaup equations.

Received: April 26, 2025. Revised: June 25, 2025. Accepted: August 28, 2025. Published: December 17, 2025.

1 Introduction

Fractional calculus extends the concept of differentiation and integration to non-integer orders, offering a flexible mathematical framework to describe complex physical phenomena that exhibit memory and hereditary characteristics. Since the first reference to fractional derivatives by Leibniz in 1695, this field has evolved significantly, attracting growing attention in applied mathematics, physics, biology, engineering, and economics due to its ability to describe nonlocal and time-dependent dynamics, [**1**],[**2**],[**3**].

Researchers have introduced multiple definitions of fractional operators, including, [**4**],[**5**],[**6**]. Among them, the Caputo definition is particularly suitable for physical modeling because it allows the use of classical initial conditions and ensures that the derivative of a constant is zero. However, solving nonlinear fractional partial differential equations (NFPDEs) remains a challenging task since analytical solutions are rarely available.

To overcome this difficulty, numerous semi-analytical and numerical techniques have been developed, such as the Adomian Decomposition Method (ADM), [**7**], the Variational Iteration Method (VIM), [**8**], the Optimal Homotopy Asymptotic Method (OHAM), [**9**], the Quintic B-Spline Method, [**10**], the New Iterative Method (NIM), [**11**], and the Fractional Residual Power Series Method (FRPSM), [**12**]. In recent years, researchers have increasingly combined transformation techniques with numerical approaches to improve convergence and computational efficiency. For instance, [**13**], proposed the Laplace Residual Power Series Method (L-RPSM), which merges the Laplace transform with the residual power series framework to generate highly accurate and rapidly convergent approximations for fractional systems, [**14**], [**15**], [**16**].

Recent studies in fractional dynamics and advanced computational methods, [**17**], [**18**], [**19**], [**20**], further emphasize the growing demand for robust and flexible analytical tools to address nonlinear time-fractional models. Building upon these developments, the present study adopts the L-RPSM as a novel and efficient framework that combines the strengths of the Laplace transform and the Residual Power Series Method to enhance numerical analysis and approximation accuracy for the fractional Whitham–Broer–Kaup (WBK) model. Specifically, the method is applied to the nonlinear time-fractional WBK equations, [**21**], which describe the propagation of shallow water waves with dispersive effects:

$$\begin{cases} \mathcal{D}_{\varrho}^{\alpha}\mathfrak{u}(\zeta,\varrho)+\mathfrak{u}(\zeta,\varrho)\mathcal{D}_{\zeta}\mathfrak{u}(\zeta,\varrho)+\mathcal{D}_{\zeta}\mathfrak{v}(\zeta,\varrho) \\ +\sigma\mathcal{D}_{\zeta\zeta}\mathfrak{u}(\zeta,\varrho)=0, \\ \mathcal{D}_{\varrho}^{\alpha}\mathfrak{v}(\zeta,\varrho)+\mathfrak{u}(\zeta,\varrho)\mathcal{D}_{\zeta}\mathfrak{v}(\zeta,\varrho)+\mathfrak{v}(\zeta,\varrho)\mathcal{D}_{\zeta}\mathfrak{u}(\zeta,\varrho) \\ +\delta\mathcal{D}_{\zeta\zeta\zeta}\mathfrak{u}(\zeta,\varrho)-\sigma\mathcal{D}_{\zeta\zeta}\mathfrak{v}(\zeta,\varrho)=0, \\ \zeta\in\mathbb{R},\varrho\in[0,T],\alpha\in(0,1] \end{cases}$$

Here, $\mathfrak{u}(\zeta,\varrho)$ denotes the horizontal velocity, $\mathfrak{v}(\zeta,\varrho)$ describes the deviation of the height from its equilibrium position, and σ and δ are real constants related to different diffusion rates.

The proposed method combines the Laplace transform with the residual power series framework to efficiently generate approximate solutions and to investigate the influence of the fractional order on the system behavior. The obtained results demonstrate that the proposed approach is simple to implement, highly accurate, and rapidly convergent, making it applicable to a wide range of nonlinear fractional models.

The following sections provide a comprehensive and detailed description of our methodology. Section 2 presents the essential background information necessary to understand the fractional Caputo derivative and the fractional Laplace transform. Section 3 outlines the steps involved in applying the L-RPSM to solve the nonlinear time-fractional WBK equations. In Section 4, a numerical application is analyzed to demonstrate the effectiveness, accuracy, and convergence of the proposed method. Finally, Section 5 summarizes the main findings and contributions of the paper, emphasizing the significance of the L-RPSM in advancing the study of nonlinear fractional partial differential equations.

2 Basic Concepts

To lay the groundwork for the subsequent study, this section presents the fundamental concepts of fractional calculus used throughout the paper. In particular, we focus on the Caputo fractional derivative, the Riemann–Liouville fractional integral, and the fractional Laplace transform, together with some of their essential properties.

Definition 1. *[**5**] The Caputo fractional derivative for order α ($\alpha > 0$) of $\mathfrak{u}(\zeta,\varrho)$ is given by:*

$$\mathcal{D}_{\varrho}^{\alpha}\mathfrak{u}(\zeta,\varrho)=\begin{cases} \mathcal{I}_{\varrho}^{n-\alpha}(d_{\varrho}^{n}u(\zeta,\varrho)),\ n-1<\alpha<n, \\ d_{\varrho}^{n}u(\zeta,\varrho),\ \alpha=n\in\mathbb{N}. \end{cases}$$

where $\varrho \geq 0$, $\zeta \in J$(J is an interval), $d^n_\varrho = \dfrac{d^n}{d\varrho^n}$ and $\mathcal{I}^\beta_\varrho$ is the Riemann-Liouville fractional integral of order β that denoted by:

$$\mathcal{I}^\beta_\varrho \mathfrak{u}(\zeta,\varrho) = \begin{cases} \frac{1}{\Gamma(\beta)} & \int_0^\varrho (\varrho-\tau)^{\beta-1}\mathfrak{u}(\zeta,\varrho)d\zeta, \\ & \beta>0,\ 0\leq\tau<\varrho, \\ & u(\zeta,\varrho), \quad \beta=0. \end{cases}$$

Definition 2. [22] *Let $\mathfrak{u}$ is a piecewise continuous (PC) function on $J\times[0;\infty)$ and of exponential order λ, then the Laplace transformation (LT) of $\mathfrak{u}(\zeta,\varrho)$ is expressed as follows:*

$$\mathcal{U}(\zeta,\mathfrak{s}) = \mathcal{L}\left[\mathfrak{u}(\zeta,\varrho)\right] = \int_0^{+\infty} e^{-\mathfrak{s}\varrho}\mathfrak{u}(\zeta,\varrho)d\varrho, \quad Re(\mathfrak{s})>\lambda,$$

and the inverse LT of $\mathcal{U}(\zeta,\mathfrak{s})$ is defined by:

$$\mathfrak{u}(\zeta,\varrho) = \mathcal{L}^{-1}\left[\mathcal{U}(\zeta,\mathfrak{s})\right] = \int_{l-i\infty}^{l+i\infty} e^{\mathfrak{s}\varrho}\mathfrak{u}(\zeta,\mathfrak{s})d\mathfrak{s}, \quad l=Re(\mathfrak{s})>l_0,$$

where l_0 sits in the region of the right half-plane where the integral converges.

Lemma 1. [23] *Let $\mathfrak{u}$ and $\mathfrak{v}$ be piecewise continuous (PC) functions defined on $J\times[0,+\infty)$, with exponential orders λ_1 and λ_2, respectively, such that $\lambda_1<\lambda_2$. Denote their Laplace transforms by $\mathcal{U}(\zeta,\mathfrak{s}) = \mathcal{L}\left[\mathfrak{u}(\zeta,\varrho)\right]$ and $\mathcal{V}(\zeta,\mathfrak{s}) = \mathcal{L}\left[\mathfrak{v}(\zeta,\varrho)\right]$. Then, the following properties hold:*

- $\mathcal{L}\left[a\mathfrak{u}(\zeta,\varrho)+b\mathfrak{v}(\zeta,\varrho)\right] = a\mathcal{U}(\zeta,\mathfrak{s})+b\mathcal{V}(\zeta,\mathfrak{s})$, $\zeta\in J,\ \ \mathfrak{s}>\lambda_1,\ \ a,b\in\mathbb{R}$.
- $\lim\limits_{\mathfrak{s}\longrightarrow+\infty}\mathcal{V}(\zeta,\mathfrak{s}) = \mathfrak{v}(\zeta,0), \quad \zeta\in J.$
- $\mathcal{L}\left[I^\alpha_\varrho\mathfrak{u}(\zeta,\varrho)\right] = \dfrac{\mathcal{U}(\zeta,\mathfrak{s})}{\mathfrak{s}^\alpha}, \ \ \alpha>0$
- $\mathcal{L}\left[\mathcal{D}^\alpha_\varrho\mathfrak{u}(\zeta,\varrho)\right] = \mathfrak{s}^\alpha\mathcal{U}(\zeta,\mathfrak{s}) - \sum_{k=0}^{m-1}\mathfrak{s}^{\alpha-k-1}\mathfrak{u}^k(\zeta,0),\ \ m-1<\alpha\leq m$
- $\mathcal{L}\left[\mathcal{D}^{n\alpha}_\varrho\mathfrak{u}(\zeta,\varrho)\right] = \mathfrak{s}^{n\alpha}\mathcal{U}(\zeta,\mathfrak{s}) - \sum_{k=0}^{n-1}\mathfrak{s}^{(n-k)\alpha-1}\mathcal{D}^{k\alpha}_\varrho\mathfrak{u}(\zeta,0), \quad 0<\alpha\leq1$, *where* $\mathcal{D}^{n\alpha}_\varrho = \mathcal{D}^\alpha_t.\mathcal{D}^\alpha_\varrho...\mathcal{D}^\alpha_\varrho(n-times)$.

Theorem 1. *Let $\mathfrak{u}$ be a PC function on $J\times[0;\infty)$ and of exponential order λ.*
Assume that the fractional expansion of $\mathcal{U}(\zeta,\mathfrak{s}) = \mathcal{L}\left[\mathfrak{u}(\zeta,\varrho)\right]$ is given as follows:

$$\mathcal{U}(\zeta,\mathfrak{s}) = \sum_{n=0}^{+\infty}\frac{a_n(\zeta)}{\mathfrak{s}^{n\alpha+1}}, \quad 0<\alpha\leq1, \quad \zeta\in J, \quad \mathfrak{s}>\lambda, \tag{1}$$

then $a_n(\zeta) = \mathcal{D}^{n\alpha}_\varrho\mathfrak{u}(\zeta,0)$ and inverse LT of the expansion (1) has the following formula:

$$\mathfrak{u}(\zeta,\varrho) = \sum_{n=0}^{+\infty}\frac{\mathcal{D}^{n\alpha}_\varrho\mathfrak{u}(\zeta,0)}{\Gamma(n\alpha+1)}\varrho^{n\alpha}, \quad 0<\alpha\leq1, \quad t\geq0.$$

3 L-RPSM for Solving the Time-Fractional WBK Equations

In this section, the L-RPSM is employed to construct approximate solutions of the time-fractional WBK equations. By transforming the system into the Laplace domain and expanding in fractional power series, the unknown coefficients are systematically determined through residual functions. The system is represented as follows:

$$\begin{cases} \mathcal{D}^\alpha_\varrho\mathfrak{u}(\zeta,\varrho)+\mathfrak{u}(\zeta,\varrho)\mathcal{D}_\zeta\mathfrak{u}(\zeta,\varrho)+\mathcal{D}_\zeta\mathfrak{v}(\zeta,\varrho) \\ +\sigma\mathcal{D}_{\zeta\zeta}\mathfrak{u}(\zeta,\varrho)=0, \\ \mathcal{D}^\alpha_\varrho\mathfrak{v}(\zeta,\varrho)+\mathfrak{u}(\zeta,\varrho)\mathcal{D}_\zeta\mathfrak{v}(\zeta,\varrho)+\mathfrak{v}(\zeta,\varrho)\mathcal{D}_\zeta\mathfrak{u}(\zeta,\varrho) \\ +\delta\mathcal{D}_{\zeta\zeta\zeta}\mathfrak{u}(\zeta,\varrho)-\sigma\mathcal{D}_{\zeta\zeta}\mathfrak{v}(\zeta,\varrho)=0, \\ \zeta\in\mathbb{R},\varrho\in[0,T],\alpha\in(0,1] \end{cases} \tag{2}$$

with the initial condition:

$$\begin{cases} \mathfrak{u}(\zeta,0)=\varphi(\zeta), \\ \mathfrak{v}(\zeta,0)=\psi(\zeta). \end{cases} \tag{3}$$

The following procedure is applied to obtain the L-RPSM solution for the IVP (2)-(3):

First, we apply the LT on both sides of equations in system (2) :

$$\begin{cases} \mathcal{L}\left[\mathcal{D}^\alpha_\varrho\mathfrak{u}(\zeta,\varrho)\right]+\mathcal{L}\left[\mathfrak{u}(\zeta,\varrho)\mathcal{D}_\zeta\mathfrak{u}(\zeta,\varrho)\right]+\mathcal{L}\left[\mathcal{D}_\zeta\mathfrak{v}(\zeta,\varrho)\right] \\ +\sigma\mathcal{L}\left[\mathcal{D}_{\zeta\zeta}\mathfrak{u}(\zeta,\varrho)\right]=0, \\ \mathcal{L}\left[\mathcal{D}^\alpha_\varrho\mathfrak{v}(\zeta,\varrho)\right]+\mathcal{L}\left[\mathfrak{u}(\zeta,\varrho)\mathcal{D}_\zeta\mathfrak{v}(\zeta,\varrho)\right] \\ +\mathcal{L}\left[\mathfrak{v}(\zeta,\varrho)\mathcal{D}_\zeta\mathfrak{u}(\zeta,\varrho)\right]+\delta\mathcal{L}\left[\delta\mathcal{D}_{\zeta\zeta\zeta}\mathfrak{u}(\zeta,\varrho)\right] \\ -\sigma\mathcal{L}\left[\mathcal{D}_{\zeta\zeta}\mathfrak{v}(\zeta,\varrho)\right]=0. \end{cases}$$

Second, according to Lemma 1, we get:

$$\begin{cases} \mathcal{L}\left[\mathcal{D}^\alpha_\varrho\mathfrak{u}(\zeta,\varrho)\right]=s^\alpha\mathcal{L}\left[\mathfrak{u}(\zeta,\varrho)\right]-s^{\alpha-1}\mathfrak{u}(\zeta,0), \\ \mathcal{L}\left(\mathcal{D}^\alpha_\varrho\mathfrak{v}(\zeta,\varrho)\right)=s^\alpha\mathcal{L}(\left[\mathfrak{v}(\zeta,\varrho)\right))-s^{\alpha-1}\mathfrak{v}(\zeta,0), \end{cases}$$

as well as using the initial condition (3), we can create a new system:

$$\begin{cases} \mathcal{U}(\zeta,\mathfrak{s})=\frac{\varphi(\zeta)}{\mathfrak{s}}-\frac{1}{\mathfrak{s}^\alpha}\mathcal{L}\left[\mathcal{L}^{-1}\left[\mathcal{U}(\zeta,\mathfrak{s})\right]\mathcal{L}^{-1}\left[\mathcal{D}_\zeta\mathcal{U}(\zeta,\mathfrak{s})\right]\right] \\ -\frac{1}{\mathfrak{s}^\alpha}\mathcal{D}_\zeta\mathcal{V}(\zeta,\mathfrak{s})-\frac{\sigma}{\mathfrak{s}^\alpha}\mathcal{D}_{\zeta\zeta}\mathcal{U}(\zeta,\mathfrak{s}), \\ \mathcal{V}(\zeta,\mathfrak{s})=\frac{\psi(\zeta)}{\mathfrak{s}}-\frac{1}{\mathfrak{s}^\alpha}\mathcal{L}\left[\mathcal{L}^{-1}\left[\mathcal{U}(\zeta,\mathfrak{s})\right]\mathcal{L}^{-1}\left[\mathcal{D}_\zeta\mathcal{V}(\zeta,\mathfrak{s})\right]\right] \\ -\frac{1}{\mathfrak{s}^\alpha}\mathcal{L}\left[\mathcal{L}^{-1}\left[\mathcal{V}(\zeta,\mathfrak{s})\right]\mathcal{L}^{-1}\left[\mathcal{D}_\zeta\mathcal{U}(\zeta,\mathfrak{s})\right]\right]-\frac{\delta}{\mathfrak{s}^\alpha}\mathcal{D}_{\zeta\zeta\zeta}\mathcal{U}(\zeta,\mathfrak{s}) \\ +\frac{\sigma}{\mathfrak{s}^\alpha}\mathcal{D}_{\zeta\zeta}\mathcal{V}(\zeta,\mathfrak{s}). \end{cases} \tag{4}$$

where $\mathcal{U}(\zeta,\mathfrak{s}) = \mathcal{L}(\mathfrak{u}(\zeta,\varrho))$ and $\mathcal{V}(\zeta,\mathfrak{s}) = \mathcal{L}(\mathfrak{v}(\zeta,\varrho))$.

After that, by using Theorem 1 and the initial condition (3), we express the approximate solution $(\mathcal{U}(\zeta,\mathfrak{s}),\mathcal{V}(\zeta,\mathfrak{s}))$ of system (4) as the following:

$$\begin{cases} \mathcal{U}(\zeta,\mathfrak{s}) = \dfrac{\varphi(\zeta)}{\mathfrak{s}} + \sum_{n=1}^{\infty} \frac{a_n(\zeta)}{\mathfrak{s}^{n\alpha+1}}, \\ \mathcal{V}(\zeta,\mathfrak{s}) = \dfrac{\psi(\zeta)}{\mathfrak{s}} + \sum_{n=1}^{\infty} \frac{b_n(\zeta)}{\mathfrak{s}^{n\alpha+1}}, \end{cases}$$

and the kth-truncated series solution of system (4) is represented as:

$$\begin{cases} \mathcal{U}_k(\zeta,\mathfrak{s}) = \dfrac{\varphi(\zeta)}{\mathfrak{s}} + \sum_{n=1}^{k} \frac{a_n(\zeta)}{\mathfrak{s}^{n\alpha+1}}, \\ \mathcal{V}_k(\zeta,\mathfrak{s}) = \dfrac{\psi(\zeta)}{\mathfrak{s}} + \sum_{n=1}^{k} \frac{b_n(\zeta)}{\mathfrak{s}^{n\alpha+1}}. \end{cases}$$

Now, we define the laplace residual functions (L-RF), $\mathcal{L}Res1$ and $\mathcal{L}Res2$, for system (4) by:

$$\begin{cases} \mathcal{L}Res1\,(\zeta,\mathfrak{s}) & = \mathcal{U}(\zeta,\mathfrak{s}) - \frac{\varphi(\zeta)}{\mathfrak{s}} \\ & + \frac{1}{\mathfrak{s}^{\alpha}}\mathcal{L}\left[\mathcal{L}^{-1}\left[\mathcal{U}(\zeta,\mathfrak{s})\right]\mathcal{L}^{-1}\left[\mathcal{D}_\zeta\mathcal{U}(\zeta,\mathfrak{s})\right]\right] \\ & + \frac{1}{\mathfrak{s}^{\alpha}}\mathcal{D}_\zeta\mathcal{V}(\zeta,\mathfrak{s}) + \frac{\sigma}{\mathfrak{s}^{\alpha}}\mathcal{D}_{\zeta\zeta}\mathcal{U}(\zeta,\mathfrak{s}), \\ \mathcal{L}Res2\,(\zeta,\mathfrak{s}) & = \mathcal{V}(\zeta,\mathfrak{s}) - \frac{\psi(\zeta)}{\mathfrak{s}} \\ & + \frac{1}{\mathfrak{s}^{\alpha}}\mathcal{L}\left[\mathcal{L}^{-1}\left[\mathcal{U}(\zeta,\mathfrak{s})\right]\mathcal{L}^{-1}\left[\mathcal{D}_\zeta\mathcal{V}(\zeta,\mathfrak{s})\right]\right] \\ & + \frac{1}{\mathfrak{s}^{\alpha}}\mathcal{L}\left[\mathcal{L}^{-1}\left[\mathcal{V}(\zeta,\mathfrak{s})\right]\mathcal{L}^{-1}\left[\mathcal{D}_\zeta\mathcal{U}(\zeta,\mathfrak{s})\right]\right] \\ & + \frac{\delta}{\mathfrak{s}^{\alpha}}\mathcal{D}_{\zeta\zeta\zeta}\mathcal{U}(\zeta,\mathfrak{s}) - \frac{\sigma}{\mathfrak{s}^{\alpha}}\mathcal{D}_{\zeta\zeta}\mathcal{V}(\zeta,\mathfrak{s}), \end{cases}$$

where $\mathcal{L}Res1_k$ and $\mathcal{L}Res2_k$ take the following forms:

$$\begin{cases} \mathcal{L}Res1_k\,(\zeta,\mathfrak{s}) & = \mathcal{U}_k(\zeta,\mathfrak{s}) - \frac{\varphi(\zeta)}{\mathfrak{s}} \\ & + \frac{1}{\mathfrak{s}^{\alpha}}\mathcal{L}\left[\mathcal{L}^{-1}\left[\mathcal{U}_k(\zeta,\mathfrak{s})\right]\mathcal{L}^{-1}\left[\mathcal{D}_\zeta\mathcal{U}_k(\zeta,\mathfrak{s})\right]\right] \\ & + \frac{1}{\mathfrak{s}^{\alpha}}\mathcal{D}_\zeta\mathcal{V}_k(\zeta,\mathfrak{s}) + \frac{\sigma}{\mathfrak{s}^{\alpha}}\mathcal{D}_{\zeta\zeta}\mathcal{U}_k(\zeta,\mathfrak{s}), \\ \mathcal{L}Res2_k\,(\zeta,\mathfrak{s}) & = \mathcal{V}_k(\zeta,\mathfrak{s}) - \frac{\psi(\zeta)}{\mathfrak{s}} \\ & + \frac{1}{\mathfrak{s}^{\alpha}}\mathcal{L}\left[\mathcal{L}^{-1}\left[\mathcal{U}_k(\zeta,\mathfrak{s})\right]\mathcal{L}^{-1}\left[\mathcal{D}_\zeta\mathcal{V}_k(\zeta,\mathfrak{s})\right]\right] \\ & + \frac{1}{\mathfrak{s}^{\alpha}}\mathcal{L}\left[\mathcal{L}^{-1}\left[\mathcal{V}_k(\zeta,\mathfrak{s})\right]\mathcal{L}^{-1}\left[\mathcal{D}_\zeta\mathcal{U}_k(\zeta,\mathfrak{s})\right]\right] \\ & + \frac{\delta}{\mathfrak{s}^{\alpha}}\mathcal{D}_{\zeta\zeta\zeta}\mathcal{U}_k(\zeta,\mathfrak{s}) - \frac{\sigma}{\mathfrak{s}^{\alpha}}\mathcal{D}_{\zeta\zeta}\mathcal{V}_k(\zeta,\mathfrak{s}). \end{cases}$$

Remark 1. *The L-RPSM possesses a number of key properties similar to those of the standard residual power series method, including:*

- $\mathcal{L}Res(\zeta,\mathfrak{s}) = 0$ *and* $\lim\limits_{k\to+\infty} \mathcal{L}Res_k(\zeta,\mathfrak{s}) = \mathcal{L}Res(\zeta,\mathfrak{s})$, *for* $\mathfrak{s} > 0$.
- $\lim\limits_{\mathfrak{s}\to+\infty} \mathfrak{s}\mathcal{L}Res(\zeta,\mathfrak{s}) = \lim\limits_{\mathfrak{s}\to+\infty} \mathfrak{s}\mathcal{L}Res_k(\zeta,\mathfrak{s}) = 0.$
- $\lim\limits_{\mathfrak{s}\to+\infty} \mathfrak{s}^{k\alpha+1}\mathcal{L}Res(\zeta,\mathfrak{s}) = \lim\limits_{\mathfrak{s}\to+\infty} \mathfrak{s}^{k\alpha+1}\mathcal{L}Res_k(\zeta,\mathfrak{s}) = 0, \quad 0 < \alpha \leq 1$ *and* $k = 0, 1, 2, ...$

Next, the first unknown coefficients, $a_1(\zeta)$ and $b_1(\zeta)$ can be determined by substituting the first-order truncated series solutions:

$$\begin{cases} \mathcal{U}_1\,(\zeta,\mathfrak{s}) = \frac{\varphi(\zeta)}{\mathfrak{s}} + \frac{a_1}{\mathfrak{s}^{\alpha+1}}, \\ \mathcal{V}_1\,(\zeta,\mathfrak{s}) = \frac{\psi(\zeta)}{\mathfrak{s}} + \frac{b_1}{\mathfrak{s}^{\alpha+1}}, \end{cases}$$

into the first L-RF, so we obtain:

$$\begin{cases} \mathcal{L}Res1_1\,(\zeta,\mathfrak{s}) & = a_1(\zeta) + \varphi(\zeta)\mathcal{D}_\zeta\varphi(\zeta) + s^{-\alpha}a_1(\zeta)\mathcal{D}_\zeta\varphi(\zeta) \\ & +\mathcal{D}_\zeta\psi(\zeta) + s^{-\alpha}\varphi(\zeta)\mathcal{D}_\zeta a_1(\zeta) + \sigma\mathcal{D}_{\zeta\zeta}\varphi(\zeta) \\ & + \frac{s^{-2\alpha}\Gamma(1+2\alpha)a_1(\zeta)\mathcal{D}_\zeta a_1(\zeta)}{\Gamma(1+\alpha)^2} + s^{-\alpha}\mathcal{D}_\zeta b_1(\zeta) + \sigma \\ & \times s^{-\alpha}\mathcal{D}_{\zeta\zeta}a_1(\zeta), \\ \mathcal{L}Res2_1\,(\zeta,\mathfrak{s}) & = \frac{\Gamma(2\alpha+1)b_1(\zeta)s^{-2\alpha}\mathcal{D}_\zeta a_1(\zeta)}{\Gamma(\alpha+1)^2} + \delta\mathcal{D}_{\zeta\zeta\zeta}a_1(\zeta)s^{-\alpha} \\ & + \frac{a_1(\zeta)\Gamma(2\alpha+1)s^{-2\alpha}\mathcal{D}_\zeta b_1(\zeta)}{\Gamma(\alpha+1)^2} + a_1(\zeta)s^{-\alpha}\mathcal{D}_\zeta\psi(\zeta) \\ & +s^{-\alpha}\psi(\zeta)\mathcal{D}_\zeta a_1(\zeta) - \sigma s^{-\alpha}\mathcal{D}_{\zeta\zeta}b_1(\zeta) + b_1(\zeta) \\ & \times s^{-\alpha}\mathcal{D}_\zeta\varphi(\zeta) + s^{-\alpha}\varphi(\zeta)\mathcal{D}_\zeta b_1(\zeta) + b_1(\zeta) + l \\ & \times\mathcal{D}_{\zeta\zeta\zeta}\varphi(\zeta) - \sigma\mathcal{D}_{\zeta\zeta}\psi(\zeta) + \psi(\zeta)\mathcal{D}_\zeta\varphi(\zeta) + \varphi(\zeta) \\ & \times\mathcal{D}_\zeta\psi(\zeta), \end{cases}$$

For clarification, we recall that the limit

$$\lim_{s\to+\infty} \mathcal{L}Res_k(\zeta,s)$$

in the Laplace domain is taken with respect to the Laplace variable s, and its existence is guaranteed under the standard assumption that the transformed function is of finite exponential order. This ensures mathematical rigor and the validity of the limiting operations used in the derivation steps.

Therefore, by using $\lim\limits_{\mathfrak{s}\longrightarrow\infty} \mathfrak{s}^{\alpha+1}\mathcal{L}Res1_1\,(\zeta,\mathfrak{s}) = 0$ and $\lim\limits_{\mathfrak{s}\longrightarrow\infty} \mathfrak{s}^{\alpha+1}\mathcal{L}Res2_1\,(\zeta,\mathfrak{s}) = 0$, we get:

$$\begin{cases} a_1\,(\zeta) & = -\sigma\mathcal{D}_{\zeta\zeta}\varphi(\zeta) - \varphi(\zeta)\mathcal{D}_\zeta\varphi(\zeta) - \mathcal{D}_\zeta\psi(\zeta), \\ b_1\,(\zeta) & = -\delta\mathcal{D}_{\zeta\zeta\zeta}\varphi(\zeta) + \sigma\mathcal{D}_{\zeta\zeta}\psi(\zeta) \\ & \quad -\psi(\zeta)\mathcal{D}_\zeta\varphi(\zeta) - \varphi(\zeta)\mathcal{D}_\zeta\psi(\zeta), \end{cases}$$

Then, we find the 1st-approximate solution of system (4) as:

$$\begin{cases} \mathcal{U}_1(\zeta,\mathfrak{s}) & = \frac{\varphi(\zeta)}{\mathfrak{s}} + \frac{-\sigma\mathcal{D}_{\zeta\zeta}\varphi(\zeta) - \varphi(\zeta)\mathcal{D}_\zeta\varphi(\zeta) - \mathcal{D}_\zeta\psi(\zeta)}{\mathfrak{s}^{\alpha+1}}, \\ \mathcal{V}_1(\zeta,\mathfrak{s}) & = \frac{\psi(\zeta)}{\mathfrak{s}} + \frac{-\delta\mathcal{D}_{\zeta\zeta\zeta}\varphi(\zeta) + \sigma\mathcal{D}_{\zeta\zeta}\psi(\zeta) - \psi(\zeta)\mathcal{D}_\zeta\varphi(\zeta) - \varphi(\zeta)\mathcal{D}_\zeta\psi(\zeta)}{\mathfrak{s}^{\alpha+1}}. \end{cases}$$

Employing the previously mentioned steps, we acquire:

$$\begin{cases} a_2(\zeta) & = \delta\mathcal{D}_{\zeta\zeta\zeta\zeta}\varphi(\zeta) + \sigma^2\mathcal{D}_{\zeta\zeta\zeta\zeta}\varphi(\zeta) + 2\sigma\varphi(\zeta)\mathcal{D}_{\zeta\zeta\zeta}\varphi(\zeta) \\ & +4\sigma\mathcal{D}_\zeta\varphi(\zeta)\mathcal{D}_{\zeta\zeta}\varphi(\zeta) + \psi(\zeta)\mathcal{D}_{\zeta\zeta}\varphi(\zeta) + \varphi(\zeta)^2\mathcal{D}_{\zeta\zeta}\varphi(\zeta) \\ & +3\mathcal{D}_\zeta\varphi(\zeta)\mathcal{D}_\zeta\psi(\zeta) + 2\varphi(\zeta)\mathcal{D}_\zeta\varphi(\zeta)^2 + 2\varphi(\zeta)\mathcal{D}_{\zeta\zeta}\psi(\zeta), \\ b_2(\zeta) & = 2\delta\varphi(\zeta)\mathcal{D}_{\zeta\zeta\zeta\zeta}\varphi(\zeta) + 3\delta\mathcal{D}_{\zeta\zeta}\varphi(\zeta)^2 + 5\delta\mathcal{D}_{\zeta\zeta\zeta}\varphi(\zeta) \\ & \times\mathcal{D}_\zeta\varphi(\zeta) + \delta\mathcal{D}_{\zeta\zeta\zeta\zeta}\psi(\zeta) + \sigma^2\mathcal{D}_{\zeta\zeta\zeta\zeta}\psi(\zeta) - 2\sigma\mathcal{D}_{\zeta\zeta}\varphi(\zeta) \\ & \times\mathcal{D}_\zeta\psi(\zeta) - 4\sigma\mathcal{D}_\zeta\varphi(\zeta)\mathcal{D}_{\zeta\zeta}\psi(\zeta) - 2\sigma\varphi(\zeta)\mathcal{D}_{\zeta\zeta\zeta}\psi(\zeta) \\ & +2\varphi(\zeta)\psi(\zeta)\mathcal{D}_{\zeta\zeta}\varphi(\zeta) + 4\varphi(\zeta)\mathcal{D}_\zeta\varphi(\zeta)\mathcal{D}_\zeta\psi(\zeta) + 2\psi(\zeta) \\ & \times\mathcal{D}_\zeta\varphi(\zeta)^2 + \varphi(\zeta)^2\mathcal{D}_{\zeta\zeta}\psi(\zeta) + \psi(\zeta)\mathcal{D}_{\zeta\zeta}\psi(\zeta) + \mathcal{D}_\zeta\psi(\zeta)^2. \\ . & \\ . & \\ . & \end{cases}$$

It follows that the L-RPS solution of system (4) is:

$$\begin{cases} \mathcal{U}(\zeta,\mathfrak{s}) & = \frac{\varphi(\zeta)}{s} + \frac{1}{s^{\alpha+1}}\Big(- \sigma\mathcal{D}_{\zeta\zeta}\varphi(\zeta) - \varphi(\zeta)\mathcal{D}_{\zeta}\varphi(\zeta) - \mathcal{D}_{\zeta}\psi(\zeta)\Big) \\ & + \frac{1}{s^{2\alpha+1}}\Big(\delta\mathcal{D}_{\zeta\zeta\zeta\zeta}\varphi(\zeta) + \sigma^2\mathcal{D}_{\zeta\zeta\zeta\zeta}\varphi(\zeta) + 2\sigma\varphi(\zeta)\mathcal{D}_{\zeta\zeta\zeta}\varphi(\zeta) \\ & +4\sigma\mathcal{D}_{\zeta}\varphi(\zeta)\mathcal{D}_{\zeta\zeta}\varphi(\zeta) + \psi(\zeta)\mathcal{D}_{\zeta\zeta}\varphi(\zeta) + \varphi(\zeta)^2\mathcal{D}_{\zeta\zeta}\varphi(\zeta) \\ & +3\mathcal{D}_{\zeta}\varphi(\zeta)\mathcal{D}_{\zeta}\psi(\zeta) + 2\varphi(\zeta)\mathcal{D}_{\zeta}\varphi(\zeta)^2 + 2\varphi(\zeta)\mathcal{D}_{\zeta\zeta}\psi(\zeta)\Big) \\ & + \dots \\ \mathcal{V}(\zeta,\mathfrak{s}) & = \frac{\psi(\zeta)}{s} + \frac{1}{s^{\alpha+1}}\Big(- \delta\mathcal{D}_{\zeta\zeta\zeta}\varphi(\zeta) \quad + \sigma\mathcal{D}_{\zeta\zeta}\psi(\zeta) - \psi(\zeta) \\ & \times\mathcal{D}_{\zeta}\varphi(\zeta) - \varphi(\zeta)\mathcal{D}_{\zeta}\psi(\zeta)\Big) + \frac{1}{s^{2\alpha+1}}\Big(2\delta\varphi(\zeta)\mathcal{D}_{\zeta\zeta\zeta\zeta}\varphi(\zeta) \\ & +3\delta\mathcal{D}_{\zeta\zeta}\varphi(\zeta)^2 + 5\delta\mathcal{D}_{\zeta\zeta\zeta}\varphi(\zeta)\mathcal{D}_{\zeta}\varphi(\zeta) + \delta\mathcal{D}_{\zeta\zeta\zeta\zeta}\psi(\zeta) \\ & +\sigma^2\mathcal{D}_{\zeta\zeta\zeta\zeta}\psi(\zeta) - 2\sigma\mathcal{D}_{\zeta\zeta}\varphi(\zeta)\mathcal{D}_{\zeta}\psi(\zeta) - 4\sigma\mathcal{D}_{\zeta}\varphi(\zeta) \\ & \times\mathcal{D}_{\zeta\zeta}\psi(\zeta) - 2\sigma\varphi(\zeta)\mathcal{D}_{\zeta\zeta\zeta}\psi(\zeta) + 2\varphi(\zeta)\psi(\zeta)\mathcal{D}_{\zeta\zeta}\varphi(\zeta) \\ & +4\varphi(\zeta)\mathcal{D}_{\zeta}\varphi(\zeta)\mathcal{D}_{\zeta}\psi(\zeta) + 2\psi(\zeta)\mathcal{D}_{\zeta}\varphi(\zeta)^2 + \varphi(\zeta)^2 \\ & \times\mathcal{D}_{\zeta\zeta}\psi(\zeta) + \psi(\zeta)\mathcal{D}_{\zeta\zeta}\psi(\zeta) + \mathcal{D}_{\zeta}\psi(\zeta)^2\Big) + \ \dots \end{cases} \tag{5}$$

Finally, by applying the inverse LT to both sides of equations in system (5), we can write the L-RPS solution of the IVP (2)-(3) as follows:

$$\begin{cases} \mathfrak{u}(\zeta,\varrho) = & \varphi(\zeta) + \frac{\varrho^{\alpha}}{\Gamma(\alpha+1)}\Big(- \sigma\mathcal{D}_{\zeta\zeta}\varphi(\zeta) \quad - \varphi(\zeta)\mathcal{D}_{\zeta}\varphi(\zeta) - \mathcal{D}_{\zeta}\psi(\zeta)\Big) \\ & + \frac{\varrho^{2\alpha}}{\Gamma(2\alpha+1)}\Big(\delta\mathcal{D}_{\zeta\zeta\zeta\zeta}\varphi(\zeta) + \sigma^2\mathcal{D}_{\zeta\zeta\zeta\zeta}\varphi(\zeta) + 2\sigma\varphi(\zeta)\mathcal{D}_{\zeta\zeta\zeta}\varphi(\zeta) \\ & +4\sigma\mathcal{D}_{\zeta}\varphi(\zeta)\mathcal{D}_{\zeta\zeta}\varphi(\zeta) + \psi(\zeta)\mathcal{D}_{\zeta\zeta}\varphi(\zeta) + \varphi(\zeta)^2\mathcal{D}_{\zeta\zeta}\varphi(\zeta) + 3 \\ & \times\mathcal{D}_{\zeta}\varphi(\zeta)\mathcal{D}_{\zeta}\psi(\zeta) + 2\varphi(\zeta)\mathcal{D}_{\zeta}\varphi(\zeta)^2 + 2\varphi(\zeta)\mathcal{D}_{\zeta\zeta}\psi(\zeta)\Big) \\ & + \dots \\ \mathfrak{v}(\zeta,\varrho) = & \psi(\zeta) + \frac{\varrho^{\alpha}}{\Gamma(\alpha+1)}\ \Big(- \delta\mathcal{D}_{\zeta\zeta\zeta}\varphi(\zeta) \quad + \sigma\mathcal{D}_{\zeta\zeta}\psi(\zeta) \quad - \psi(\zeta) \\ & \times\mathcal{D}_{\zeta}\varphi(\zeta) - \varphi(\zeta)\mathcal{D}_{\zeta}\psi(\zeta)\Big) + \frac{\varrho^{2\alpha}}{\Gamma(2\alpha+1)}\Big(2\delta\varphi(\zeta)\mathcal{D}_{\zeta\zeta\zeta\zeta}\varphi(\zeta) \\ & +3\delta\mathcal{D}_{\zeta\zeta}\varphi(\zeta)^2 + 5\delta\mathcal{D}_{\zeta\zeta\zeta}\varphi(\zeta)\mathcal{D}_{\zeta}\varphi(\zeta) + \delta\mathcal{D}_{\zeta\zeta\zeta\zeta}\psi(\zeta) + \sigma^2 \\ & \times\mathcal{D}_{\zeta\zeta\zeta\zeta}\psi(\zeta) - 2\sigma\mathcal{D}_{\zeta\zeta}\varphi(\zeta)\mathcal{D}_{\zeta}\psi(\zeta) - 4\sigma\mathcal{D}_{\zeta}\varphi(\zeta)\mathcal{D}_{\zeta\zeta}\psi(\zeta) \\ & -2\sigma\varphi(\zeta)\mathcal{D}_{\zeta\zeta\zeta}\psi(\zeta) + 2\varphi(\zeta)\psi(\zeta)\mathcal{D}_{\zeta\zeta}\varphi(\zeta) + 4\varphi(\zeta)\mathcal{D}_{\zeta}\varphi(\zeta) \\ & \times\mathcal{D}_{\zeta}\psi(\zeta) + 2\psi(\zeta)\mathcal{D}_{\zeta}\varphi(\zeta)^2 \quad + \varphi(\zeta)^2\mathcal{D}_{\zeta\zeta}\psi(\zeta) + \psi(\zeta) \\ & \times\mathcal{D}_{\zeta\zeta}\psi(\zeta) + \mathcal{D}_{\zeta}\psi(\zeta)^2\Big) + \ \dots \end{cases}$$

4 Analysis of Convergence

An essential aspect of any numerical method is the convergence of its approximate solutions toward the exact solution. Therefore, before proceeding to the numerical results, we present here the theoretical justification of the convergence of the proposed L-RPSM.

Theorem 2. *[12] Let $\mathfrak{u}_i(\zeta,\varrho)$, $i = 1,2$, be a piecewise continuous function (PCF) on $I \times [0,+\infty)$ and of exponential order λ. Suppose that $\mathcal{U}_i(\zeta,s) = \mathcal{L}[\mathfrak{u}_i(\zeta,\varrho)]$ can be expressed by the expansion in equation (1). If*

$$\left|s\mathcal{L}\left[D_{\varrho}^{(n+1)}\mathfrak{u}_i(\zeta,\varrho)\right]\right| \leq M(\zeta) \quad \textit{on } I \times (\lambda,\gamma],$$

then the remainder term R_n of the Laplace transform of the MFPS satisfies

$$|R_n(\zeta,s)| \leq \frac{M(\zeta)}{s^{1+(n+1)\alpha}}, \quad \zeta \in I, \quad \lambda < s \leq \gamma.$$

Theorem 3. *Assume that there exists a constant $0 < \gamma < 1$ such that*

$$\|\mathfrak{u}_{i,n+1}(\zeta,\varrho)\| \leq \gamma\|\mathfrak{u}_{i,n}(\zeta,\varrho)\|,$$
$$i = 1,2,\ \forall n \in \mathbb{N},\ \zeta \in I,\ 0 < \varrho < T.$$

Then, the sequence of approximate solutions $\{\mathfrak{u}_{i,n}\}$ converges to the exact solution $\mathfrak{u}_i(\zeta,\varrho)$.

Proof

For all $\zeta \in I$ and $0 < \varrho < T$, we have

$$\begin{aligned} \|\mathfrak{u}_i(\zeta,\varrho) - \mathfrak{u}_{i,n}(\zeta,\varrho)\| &= \left\|\sum_{k=n+1}^{+\infty}\mathfrak{u}_{i,k}(\zeta,\varrho)\right\| \\ &\leq \sum_{k=n+1}^{+\infty}\|\mathfrak{u}_{i,k}(\zeta,\varrho)\| \\ &\leq \|\phi(\zeta)\|\sum_{k=n+1}^{+\infty}\gamma^k \\ &= \frac{\gamma^{n+1}}{1-\gamma}\|\phi(\zeta)\|. \end{aligned}$$

Therefore, as $n \to \infty$,

$$\|\mathfrak{u}_i(\zeta,\varrho) - \mathfrak{u}_{i,n}(\zeta,\varrho)\| \to 0,$$

which confirms the convergence of the series.

These results confirm that the proposed L-RPSM produces a uniformly convergent series of approximate solutions, ensuring both accuracy and stability of the method before applying it to numerical examples.

5 Numerical Application

In the previous sections, the Laplace-Residual Power Series Method was presented in a general form for solving nonlinear fractional partial differential equations, including a brief convergence study to determine the number of terms needed for accurate approximations. Here, building on this general formulation and convergence analysis, we apply L-RPSM to the nonlinear time-fractional Whitham–Broer–Kaup equations to illustrate its practical implementation, accuracy, and efficiency. The objective is to verify the reliability of the method in obtaining approximate analytical solutions for fractional models that describe dispersive shallow water waves. The time-fractional WBK system considered here is given by:

$$\begin{cases} \mathcal{D}_{\varrho}^{\alpha}\mathfrak{u}(\zeta,\varrho)+\mathfrak{u}(\zeta,\varrho)\mathcal{D}_{\zeta}\mathfrak{u}(\zeta,\varrho)+\mathcal{D}_{\zeta}\mathfrak{v}(\zeta,\varrho) \\ +\frac{3}{2}\mathcal{D}_{\zeta\zeta}\mathfrak{u}(\zeta,\varrho)=0, \\ \mathcal{D}_{\varrho}^{\alpha}\mathfrak{v}(\zeta,\varrho)+\mathfrak{u}(\zeta,\varrho)\mathcal{D}_{\zeta}\mathfrak{v}(\zeta,\varrho)+\mathfrak{v}(\zeta,\varrho)\mathcal{D}_{\zeta}\mathfrak{u}(\zeta,\varrho) \\ +\frac{3}{2}\mathcal{D}_{\zeta\zeta\zeta}\mathfrak{u}(\zeta,\varrho)-\frac{3}{2}\mathcal{D}_{\zeta\zeta}\mathfrak{v}(\zeta,\varrho)=0, \end{cases} \tag{6}$$

the exact solution of system (6) at $\alpha=1$, [**16**], is :

$$\begin{cases} \mathfrak{u}(\zeta,\varrho) & =\frac{1}{200}-\frac{1}{2}\sqrt{\frac{3}{5}}\coth\left(\frac{1}{10}\left(\zeta+10-\frac{5\varrho}{1000}\right)\right), \\ \mathfrak{v}(\zeta,\varrho) & =-\frac{1}{20}\sqrt{\frac{3}{5}}\left(\frac{\sqrt{15}}{2}+\frac{3}{2}\right)\operatorname{csch}^2\Big(\frac{1}{10}\Big(\zeta+10 \\ & \quad -\frac{5\varrho}{1000}\Big)\Big), \end{cases}$$

so the initial condition is given by:

$$\begin{cases} \mathfrak{u}(\zeta,0)=\frac{1}{200}-\frac{1}{2}\sqrt{\frac{3}{5}}\coth\left(\frac{\zeta+10}{10}\right), \\ \mathfrak{v}(\zeta,0)=-\frac{1}{20}\sqrt{\frac{3}{5}}\left(\frac{\sqrt{15}}{2}+\frac{3}{2}\right)\operatorname{csch}^2\left(\frac{\zeta+10}{10}\right). \end{cases}$$

Using the L-RPSM, we determine:

$$\begin{cases} \mathcal{U}(\zeta,\mathfrak{s}) & =\frac{1}{200\mathfrak{s}}-\frac{1}{2\mathfrak{s}}\sqrt{\frac{3}{5}}\coth\left(\frac{\zeta+10}{10}\right)-\frac{1}{\mathfrak{s}^{\alpha}} \\ & \times\mathcal{L}\left[\mathcal{L}^{-1}\left[\mathcal{U}(\zeta,\mathfrak{s})\right]\mathcal{L}^{-1}\left[\mathcal{D}_{\zeta}\mathcal{U}(\zeta,\mathfrak{s})\right]\right] \\ & -\frac{1}{\mathfrak{s}^{\alpha}}\mathcal{D}_{\zeta}\mathcal{V}(\zeta,\mathfrak{s})-\frac{3}{2\mathfrak{s}^{\alpha}}\mathcal{D}_{\zeta\zeta}\mathcal{U}(\zeta,\mathfrak{s}), \\ \mathcal{V}(\zeta,\mathfrak{s}) & =-\frac{1}{20\mathfrak{s}}\sqrt{\frac{3}{5}}\left(\frac{\sqrt{15}}{2}+\frac{3}{2}\right)\operatorname{csch}^2\left(\frac{\zeta+10}{10}\right) \\ & -\frac{1}{\mathfrak{s}^{\alpha}}\mathcal{L}\left[\mathcal{L}^{-1}\left[\mathcal{U}(\zeta,\mathfrak{s})\right]\mathcal{L}^{-1}\left[\mathcal{D}_{\zeta}\mathcal{V}(\zeta,\mathfrak{s})\right]\right] \\ & -\frac{1}{\mathfrak{s}^{\alpha}}\mathcal{L}\left[\mathcal{L}^{-1}\left[\mathcal{V}(\zeta,\mathfrak{s})\right]\mathcal{L}^{-1}\left[\mathcal{D}_{\zeta}\mathcal{U}(\zeta,\mathfrak{s})\right]\right] \\ & -\frac{3}{2\mathfrak{s}^{\alpha}}\mathcal{D}_{\zeta\zeta\zeta}\mathcal{U}(\zeta,\mathfrak{s})+\frac{3}{2\mathfrak{s}^{\alpha}}\mathcal{D}_{\zeta\zeta}\mathcal{V}(\zeta,\mathfrak{s}), \end{cases} \tag{7}$$

and the kth-truncated series solution of system (7) is:

$$\begin{cases} \mathcal{U}_k(\zeta,\mathfrak{s}) & =\frac{1}{200}-\frac{1}{2}\sqrt{\frac{3}{5}}\coth\left(\frac{\zeta+10}{10}\right) \\ & \quad+\sum_{n=1}^{k}\frac{a_n(\zeta)}{\mathfrak{s}^{n\alpha+1}}, \\ \mathcal{V}_k(\zeta,\mathfrak{s}) & =-\frac{1}{20}\sqrt{\frac{3}{5}}\left(\frac{\sqrt{15}}{2}+\frac{3}{2}\right)\operatorname{csch}^2\left(\frac{\zeta+10}{10}\right) \\ & \quad+\sum_{n=1}^{k}\frac{b_n(\zeta)}{\mathfrak{s}^{n\alpha+1}}, \end{cases}$$

thus, the kth-LRF is expressed as:

$$\begin{cases} \mathcal{L}Res1_k(\zeta,\mathfrak{s}) & =\mathcal{U}_k(\zeta,\mathfrak{s})-\frac{1}{200\mathfrak{s}}+\frac{1}{2\mathfrak{s}}\sqrt{\frac{3}{5}} \\ & \coth\left(\frac{\zeta+10}{10}\right)+\frac{1}{\mathfrak{s}^{\alpha}}\mathcal{L}\Big[\mathcal{L}^{-1} \\ & \left[\mathcal{U}_k(\zeta,\mathfrak{s})\right]\mathcal{L}^{-1}\left[\mathcal{D}_{\zeta}\mathcal{U}_k(\zeta,\mathfrak{s})\right]\Big] \\ & +\frac{1}{\mathfrak{s}^{\alpha}}\mathcal{D}_{\zeta}\mathcal{V}_k(\zeta,\mathfrak{s})+\frac{3}{2\mathfrak{s}^{\alpha}}\mathcal{D}_{\zeta\zeta}\mathcal{U}_k(\zeta,\mathfrak{s}), \\ \mathcal{L}Res2_k(\zeta,\mathfrak{s}) & =\mathcal{V}_k(\zeta,\mathfrak{s})+\frac{1}{20\mathfrak{s}}\sqrt{\frac{3}{5}}\left(\frac{\sqrt{15}}{2}+\frac{3}{2}\right) \\ & \operatorname{csch}^2\left(\frac{\zeta+10}{10}\right)+\frac{1}{\mathfrak{s}^{\alpha}}\mathcal{L}\Big[\mathcal{L}^{-1}\left[\mathcal{U}_k(\zeta,\mathfrak{s})\right] \\ & \left[\mathcal{V}_k(\zeta,\mathfrak{s})\right]\mathcal{L}^{-1}\left[\mathcal{D}_{\zeta}\mathcal{U}_k(\zeta,\mathfrak{s})\right]\Big]+\frac{3}{2\mathfrak{s}^{\alpha}} \\ & \times\mathcal{D}_{\zeta\zeta\zeta}\mathcal{U}_k(\zeta,\mathfrak{s})-\frac{3}{2\mathfrak{s}^{\alpha}}\mathcal{D}_{\zeta\zeta}\mathcal{V}_k(\zeta,\mathfrak{s}). \end{cases}$$

Following the L-RPSM's steps gives:

$$a_1(\zeta)=-\frac{1}{4\times10^3}\sqrt{\frac{3}{5}}\operatorname{csch}^2\left(\frac{\zeta}{10}+1\right)$$

$$b_1(\zeta)=-\frac{3\left(\sqrt{15}+5\right)}{2\times10^5}\coth\left(\frac{\zeta}{10}+1\right)\operatorname{csch}^2\left(\frac{\zeta}{10}+1\right)$$

$$a_2(\zeta)=-\frac{1}{8\times10^6}\sqrt{\frac{3}{5}}\sinh\left(\frac{\zeta}{5}+2\right)\operatorname{csch}^4\left(\frac{\zeta}{10}+1\right)$$

$$b_2(\zeta)=-\frac{3\left(\sqrt{15}+5\right)}{4\times10^8}\operatorname{csch}^2\left(\frac{\zeta}{10}+1\right)\left(2\coth^2\left(\frac{\zeta}{10}+1\right)+\operatorname{csch}^2\left(\frac{\zeta}{10}+1\right)\right)$$

$$a_3(\zeta)=\frac{1}{4\times10^{10}\Gamma(\alpha+1)^2}\Bigg(150\Gamma(2\alpha+1)\sinh\left(\frac{\zeta}{5}+2\right)\times\operatorname{csch}^6\left(\frac{\zeta}{10}+1\right)-\Gamma(\alpha+1)^2\Bigg(\sqrt{15}\operatorname{csch}^4\left(\frac{\zeta}{10}+1\right)+2\sqrt{15}\coth^2\left(\frac{\zeta}{10}+1\right)\operatorname{csch}^2\left(\frac{\zeta}{10}+1\right)+300\sinh\left(\frac{\zeta}{5}+2\right)\operatorname{csch}^6\left(\frac{\zeta}{10}+1\right)\Bigg)\Bigg)$$

$$b_3(\zeta)=-\frac{3}{16\times10^{11}\Gamma(\alpha+1)^2}\operatorname{csch}^6\left(\frac{\zeta}{10}+1\right)\Bigg(\Gamma(\alpha+1)^2\times\Bigg(8\left(\sqrt{15}+5\right)\sinh\left(\frac{\zeta}{5}+2\right)+\left(\sqrt{15}+5\right)\times\sinh^3\left(\frac{\zeta}{5}+2\right)\operatorname{csch}^2\left(\frac{\zeta}{10}+1\right)+400\left(\sqrt{15}+3\right)\times\sinh^2\left(\frac{\zeta}{5}+2\right)\operatorname{csch}^2\left(\frac{\zeta}{10}+1\right)+400\left(\sqrt{15}+3\right)\Bigg)-\frac{200\left(\sqrt{15}+3\right)\Gamma(2\alpha+1)}{e^2}\Bigg(\left(e^4-1\right)\sinh\left(\frac{\zeta}{5}\right)+\left(1+e^4\right)\cosh\left(\frac{\zeta}{5}\right)+3e^2\Bigg)\Bigg)$$

.
.
.

Consequently, the solution of the system (7) can be expressed as:

$$
\begin{cases}
\mathcal{U}(\zeta,\mathfrak{s}) & = \frac{1}{200\mathfrak{s}} - \frac{1}{2\mathfrak{s}}\sqrt{\frac{3}{5}}\coth\left(\frac{\zeta+10}{10}\right) - \frac{1}{4\times10^{3}\mathfrak{s}^{1+\alpha}}\sqrt{\frac{3}{5}} \\
& \times\operatorname{csch}^2\left(\frac{\zeta}{10}+1\right) - \frac{1}{8\times10^{6}\mathfrak{s}^{1+2\alpha}}\sqrt{\frac{3}{5}}\sinh\left(\frac{\zeta}{5}+2\right) \\
& \times\operatorname{csch}^4\left(\frac{\zeta}{10}+1\right) + \frac{1}{4\times10^{10}\Gamma(\alpha+1)^2\mathfrak{s}^{1+3\alpha}}\Bigg(150 \\
& \times\Gamma(2\alpha+1)\sinh\left(\frac{\zeta}{5}+2\right)\operatorname{csch}^6\left(\frac{\zeta}{10}+1\right) \\
& -\Gamma(\alpha+1)^2\Bigg(\sqrt{15}\operatorname{csch}^4\left(\frac{\zeta}{10}+1\right) + 2\sqrt{15} \\
& \coth^2\left(\frac{\zeta}{10}+1\right) + \dots \\
\mathcal{V}(\zeta,\mathfrak{s}) & = -\frac{1}{20\mathfrak{s}}\sqrt{\frac{3}{5}}\left(\frac{\sqrt{15}}{2} + \frac{3}{2}\right)\operatorname{csch}^2\left(\frac{\zeta+10}{10}\right) \\
& -\frac{3\left(\sqrt{15}+5\right)}{2\times10^{5}\mathfrak{s}^{1+\alpha}}\coth\left(\frac{\zeta}{10}+1\right)\operatorname{csch}^2\left(\frac{\zeta}{10}+1\right) \\
& -\frac{3\left(\sqrt{15}+5\right)}{4\times10^{8}\mathfrak{s}^{1+2\alpha}}\operatorname{csch}^2\left(\frac{\zeta}{10}+1\right)\Bigg(2\coth^2\left(\frac{\zeta}{10}+1\right) \\
& +\operatorname{csch}^2\left(\frac{\zeta}{10}+1\right)\Bigg) - \frac{3}{16\times10^{11}\Gamma(\alpha+1)^2\mathfrak{s}^{1+3\alpha}} \\
& \times\operatorname{csch}^6\left(\frac{\zeta}{10}+1\right)\Bigg(\Gamma(\alpha+1)^2\Bigg(8\left(\sqrt{15}+5\right) \\
& \times\sinh\left(\frac{\zeta}{5}+2\right) + \left(\sqrt{15}+5\right)\sinh^3\left(\frac{\zeta}{5}+2\right) \\
& \times\operatorname{csch}^2\left(\frac{\zeta}{10}+1\right) + 400\left(\sqrt{15}+3\right) \\
& \times\sinh^2\left(\frac{\zeta}{5}+2\right)\operatorname{csch}^2\left(\frac{\zeta}{10}+1\right) + 400(\sqrt{15} \\
& +3)\Bigg) - \frac{200\left(\sqrt{15}+3\right)\Gamma(2\alpha+1)}{e^2}\Bigg(\left(e^4-1\right)\sinh\left(\frac{\zeta}{5}\right) \\
& +\left(1+e^4\right)\times\cosh\left(\frac{\zeta}{5}\right) + 3e^2\Bigg)\Bigg) + \dots
\end{cases}
$$

Finally, the solution of equation (6) derived using the L-RPSM can be expressed as follows:

$$
\begin{cases}
\mathfrak{u}(\zeta,\varrho) & = \frac{1}{200} - \frac{1}{2}\sqrt{\frac{3}{5}}\coth\left(\frac{\zeta+10}{10}\right) - \frac{\varrho^{\alpha}}{4\times10^{3}\Gamma(1+\alpha)}\sqrt{\frac{3}{5}} \\
& \times\operatorname{csch}^2\left(\frac{\zeta}{10}+1\right) - \frac{\varrho^{2\alpha}}{8\times10^{6}\Gamma(1+2\alpha)}\sqrt{\frac{3}{5}}\sinh\left(\frac{\zeta}{5}+2\right) \\
& \times\operatorname{csch}^4\left(\frac{\zeta}{10}+1\right) + \frac{\varrho^{3\alpha}}{4\times10^{10}\Gamma(\alpha+1)^2\Gamma(1+3\alpha)}\Bigg(150 \\
& \times\Gamma(2\alpha+1)\sinh\left(\frac{\zeta}{5}+2\right)\operatorname{csch}^6\left(\frac{\zeta}{10}+1\right) \\
& -\Gamma(\alpha+1)^2\Bigg(\sqrt{15}\operatorname{csch}^4\left(\frac{\zeta}{10}+1\right) + 2\sqrt{15} \\
& \times\coth^2\left(\frac{\zeta}{10}+1\right) + \dots \\
\mathfrak{v}(\zeta,\varrho) & = -\frac{1}{20}\sqrt{\frac{3}{5}}\left(\frac{\sqrt{15}}{2}+\frac{3}{2}\right)\operatorname{csch}^2\left(\frac{\zeta+10}{10}\right) - \frac{3\left(\sqrt{15}+5\right)\varrho^{\alpha}}{2\times10^{5}\Gamma(1+\alpha)} \\
& \times\coth\left(\frac{\zeta}{10}+1\right)\operatorname{csch}^2\left(\frac{\zeta}{10}+1\right) - \frac{3\left(\sqrt{15}+5\right)\varrho^{2\alpha}}{4\times10^{8}\Gamma(1+2\alpha)} \\
& \times\operatorname{csch}^2\left(\frac{\zeta}{10}+1\right)\Bigg(2\coth^2\left(\frac{\zeta}{10}+1\right) \\
& +\operatorname{csch}^2\left(\frac{\zeta}{10}+1\right)\Bigg) - \frac{3\varrho^{3\alpha}}{16\times10^{11}\Gamma(\alpha+1)^2\Gamma(1+3\alpha)} \\
& \times\operatorname{csch}^6\left(\frac{\zeta}{10}+1\right)\Bigg(\Gamma(\alpha+1)^2\Bigg(8\left(\sqrt{15}+5\right) \\
& \times\sinh\left(\frac{\zeta}{5}+2\right) + \left(\sqrt{15}+5\right)\sinh^3\left(\frac{\zeta}{5}+2\right) \\
& \times\operatorname{csch}^2\left(\frac{\zeta}{10}+1\right) + 400\left(\sqrt{15}+3\right)\sinh^2\left(\frac{\zeta}{5}+2\right) \\
& \times\operatorname{csch}^2\left(\frac{\zeta}{10}+1\right) + 400\left(\sqrt{15}+3\right)\Bigg)
\end{cases}
$$

$$
\begin{cases}
& -\frac{200\left(\sqrt{15}+3\right)\Gamma(2\alpha+1)}{e^2}\Bigg(\left(e^4-1\right)\sinh\left(\frac{\zeta}{5}\right) + \left(1+e^4\right) \\
& \times\cosh\left(\frac{\zeta}{5}\right) + 3e^2\Bigg)\Bigg) + \dots
\end{cases}
$$

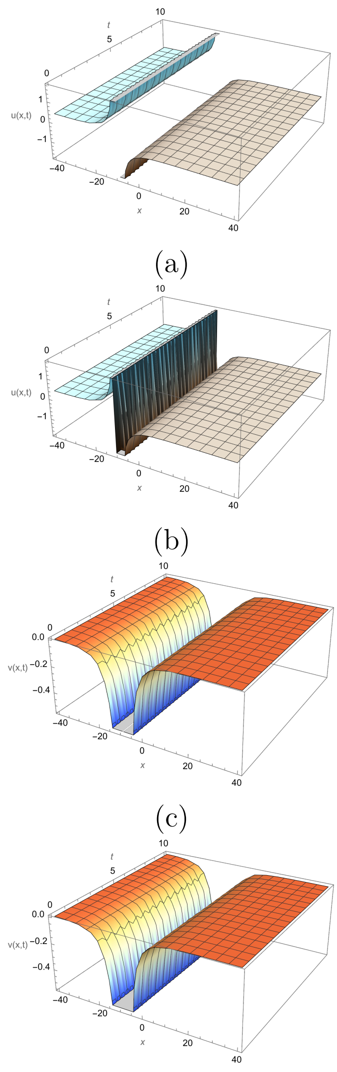

(a)

(b)

(c)

(d)

Figure 1: 3D plot of the approximate solutions obtained by the L-RPSM and their comparison with the exact solutions for $-40 \leq \zeta \leq 40$ and $0 \leq \varrho \leq 10$ at $\alpha = 1$.
(a) Exact solution $\mathfrak{u}(\zeta,\varrho)$; (b) Approximate solution $\mathfrak{u}2(\zeta,\varrho)$; (c) Exact solution $\mathfrak{v}(\zeta,\varrho)$; (d) Approximate solution $\mathfrak{v}2(\zeta,\varrho)$.
"Source: created by the authors."

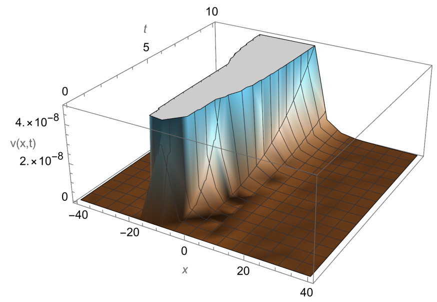

(a)

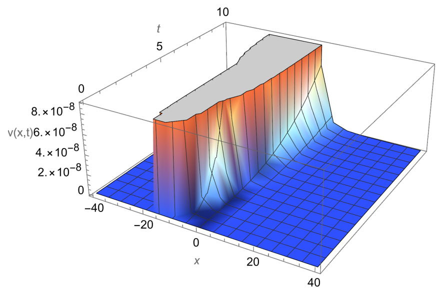

(b)

Figure 2: 3D-plots of the absolute errors with $-40 \leq \zeta \leq 40$ and $0 \leq \varrho \leq 10$ at $\alpha = 1$.
(a) $|\mathfrak{u}(\zeta, \varrho) - \mathfrak{u}_2(\zeta, \varrho)|$; (b) $|\mathfrak{v}(\zeta, \varrho) - \mathfrak{v}_2(\zeta, \varrho)|$.
"Source: created by the authors."

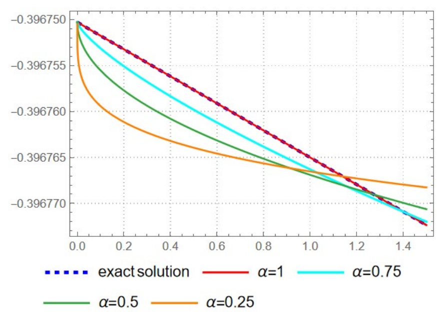

(a)

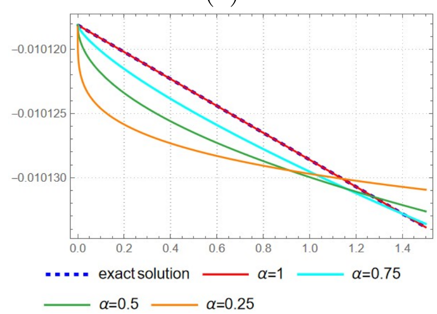

(b)

Figure 3: 2D graphs comparing the exact solutions and the 2-term L-RPSM approximate solutions for different values of α ($\alpha = 1$, $\alpha = 0.75$, $\alpha = 0.5$ and $\alpha = 0.25$) with $\zeta = 10$ and $0 \leq \varrho \leq 1.5$.
"Source: created by the authors."

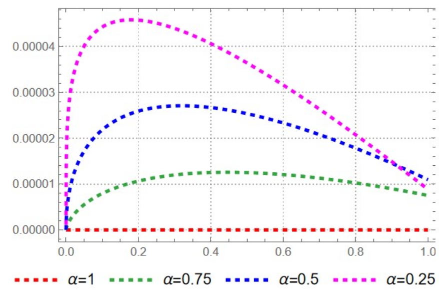

(a)

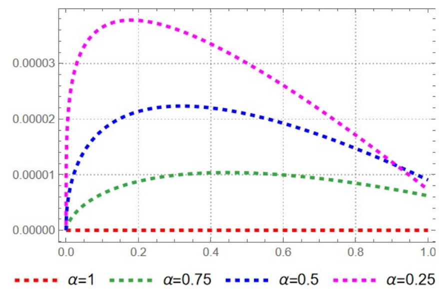

(b)

Figure 4: Absolute error distributions for the L-RPSM approximate solutions for different values of α, with $\zeta = 10$ and $0 \leq \varrho \leq 1.5$.
"Source: created by the authors."

In Appendix, Table 1 and Table 2 report the absolute errors of the L-RPSM approximate solutions $u(\zeta, \varrho)$ and $v(\zeta, \varrho)$ at different fractional orders α and various values of ζ and ϱ. The numerical data reveal that the errors are very small and decrease as α approaches unity. This behavior confirms the rapid convergence of the L-RPSM and highlights the significant influence of the fractional order α on the solution accuracy.

In Appendix, Table 3 and Table 4 provide a comparative study between the proposed L-RPSM and several well-established methods, including ADM, VIM, OHAM, B-spline, and NIM. The results clearly demonstrate the superiority of the L-RPSM, which consistently produces much smaller errors than the other methods, thereby confirming both its high accuracy and fast convergence.

Figure 1 presents the 3D plots of the exact solutions and the second-order L-RPSM approximations at $\alpha = 1$. The two surfaces almost completely overlap, indicating that the approximate solutions are practically indistinguishable from the exact ones. This strong visual agreement demonstrates the robustness and reliability of the proposed method.

Figure 2 shows the three-dimensional plots of the absolute errors at $\alpha = 1$. The errors remain extremely small across the computational domain, demonstrating that in the integer-order case, the proposed method reproduces the exact solution with remarkable accuracy and stability. The smooth error profile further confirms both the reliability and fast convergence of the L-RPSM.

Figure 3 displays the 2D solution curves for different fractional orders α. These plots clearly show the influence of fractional dynamics: as α decreases, the solutions deviate from the classical integer-order case. Lower α values slow down wave propagation and slightly reduce the amplitude, reflecting the memory effect inherent in fractional models. However, the method continues to provide stable and accurate approximations across all tested α values.

Figure 4 presents the 2D plots of the absolute errors for different fractional orders α. The errors remain extremely small throughout the computational domain, staying close to zero. The plots also highlight the influence of α on solution behavior: lower α slightly increases the error magnitude while maintaining overall stability. This demonstrates that the method maintains very high accuracy and stability for the fractional cases, while also confirming the fast convergence of the L-RPSM.

In addition to the numerical accuracy and convergence behavior discussed above, it is equally important to evaluate the computational efficiency of the proposed approach. Therefore, a brief discussion of the computational cost and runtime characteristics of the L-RPSM is provided below.

From a computational perspective, the proposed L-RPSM exhibits a remarkably low computational cost. Each term in the series is obtained analytically from the residual function without the need to recompute previous terms, which significantly reduces the overall workload. In practical terms, the number of required operations increases almost linearly with the number of series terms, while in other iterative techniques such as ADM or VIM, each new term depends on all previously computed ones, resulting in a quadratic growth of computational effort. Therefore, the L-RPSM can achieve high accuracy with fewer operations and considerably shorter runtime.

6 Conclusion

In summary, this study presents the Laplace Residual Power Series Method (L-RPSM) as a novel, systematic, and highly efficient approach for solving nonlinear time-fractional Whitham–Broer–Kaup equations. Unlike conventional techniques, which often require repeated evaluation of fractional derivatives at each iterative step and can thus be computationally demanding, the L-RPSM transforms the problem into the Laplace domain and evaluates limits at infinity, thereby simplifying the entire solution process. This transformation not only reduces computational complexity but also enhances the speed and ease of obtaining accurate approximate solutions, particularly when implemented using advanced symbolic software such as Mathematica.Through a detailed numerical application, truncation analysis, and graphical visualizations, the study demonstrates the accuracy, convergence, and robustness of the proposed method in capturing the nonlinear and fractional-order dynamics of the WBK system. Furthermore, the analysis reveals how variations in the fractional derivative order significantly affect the system's dynamics, amplitude, and propagation characteristics.Although only one representative example was presented in this study for clarity and detailed exposition, the proposed L-RPSM can be easily extended to other classes of nonlinear fractional differential equations. Even though the current numerical example employs specific hyperbolic functions for the initial conditions, the proposed L-RPSM is general and can be applied to a wide range of initial conditions while maintaining accuracy and stability. This flexibility confirms the wide applicability of the method and its potential to handle more general fractional models in future research. In addition, the L-RPSM offers a flexible and systematic framework that can be extended to higher-order approximations or applied to other fractional differential systems, highlighting its potential as a powerful tool in both theoretical and applied research.In general, the results confirm the practicality, efficiency, and broad applicability of the proposed method, paving the way for further investigations in mathematical modeling, physics, engineering, and other scientific fields where fractional-order dynamics play a vital role. Although the L-RPSM exhibits high accuracy and efficiency, it still has minor limitations. The method relies on symbolic computation of Laplace transforms, which may become challenging for strongly nonlinear or non-smooth problems. Additionally, for very small fractional orders ($\alpha \ll 1$), convergence may slow slightly due to the stiffness of the Laplace kernel. These aspects will be further investigated in future work by developing adaptive or hybrid variants of the method and by extending its application to more complex and realistic fractional systems.

Acknowledgment

The authors wish to express their sincere gratitude to Ajman University for its generous support in covering the publication fee and facilitating the completion of this research

References

[1] Barbero, G., Evangelista, L. R., Zola, R. S., Lenzi, E. K., & Scarfone, A. M. A brief review of fractional calculus as a tool for applications in physics: Adsorption phenomena and electrical impedance in complex fluids, *Fractal and Fractional*, vol. 8, no 7, 2024, pp. 369. https://doi.org/10.3390/fractalfract8070369

[2] Elsamani, S. A., Mohmmed, A. A., Kogan, K. M., Salih, S. Y. M., & Ahmed, I. A. Fractional calculus applications in engineering insights into four-dimensional chaotic systems, *J. Theory Math. Phys*, vol. 3, no 5, 2024, pp. 75-84.

[3] Cheow, Y. H., Ng, K. H., Phang, C., & Ng, K. H. The application of fractional calculus in economic growth modelling: An approach based on regression analysis, *Heliyon*, vol. 10, no 15, 2024. https://doi.org/10.1016/j.heliyon.2024.e35379

[4] Atangana, A., & Gómez-Aguilar, J. F. Numerical approximation of Riemann-Liouville definition of fractional derivative: from Riemann-Liouville to Atangana-Baleanu. *Numerical Methods for Partial Differential Equations*, vol. 34, no 5, 2017, pp. 1502-1523. https://doi.org/10.1002/num.22195

[5] Liaqat, M. I., Akgül, A., & Bayram, M. Series and closed form solution of Caputo time-fractional wave and heat problems with the variable coefficients by a novel approach, *Optical and Quantum Electronics*, vol. 56, no 2, 2024, pp. 203. https://doi.org/10.1007/s11082-023-05751-3

[6] Abro, K. A., & Atangana, A. A comparative analysis of electromechanical model of piezoelectric actuator through Caputo–Fabrizio and Atangana–Baleanu fractional derivatives. *Mathematical Methods in the Applied Sciences*, vol. 43, no 17, 2020, pp. 9681-9691. https://doi.org/10.1002/mma.6638

[7] El-Sayed, S. M., & Kaya, D. Exact and numerical traveling wave solutions of Whitham–Broer–Kaup equations, *Applied Mathematics and Computation*, vol. 167, no 2, 2005, pp. 1339-1349. https://doi.org/10.1016/j.amc.2004.08.012

[8] Rafei, M., & Daniali, H. Application of the variational iteration method to the Whitham–Broer–Kaup equations, *Computers & Mathematics with Applications*, vol. 54, no 7-8, 2007, pp. 1079-1085. https://doi.org/10.1016/j.camwa.2006.12.054

[9] Haq, S., & Ishaq, M. Solution of coupled Whitham–Broer–Kaup equations using optimal homotopy asymptotic method, *Ocean engineering*, vol. 84, 2014, pp. 81-88. https://doi.org/10.1016/j.oceaneng.2014.03.031

[10] Hadhoud, A. R., & Rageh, A. A. Redefined Quintic B-Spline Collocation Method to Solve the Time-Fractional Whitham-Broer-Kaup Equations, *Computational and Mathematical Methods* vol. 2024, no 1, 2024, pp. 7326616. https://doi.org/10.1155/2024/7326616

[11] Nawaz, R., Kumam, P., Farid, S., Shutaywi, M., Shah, Z., & Deebani, W. Application of new iterative method to time fractional Whitham–Broer–Kaup equations, *Frontiers in Physics*, vol. 8, 2020, pp. 104. https://doi.org/10.3389/fphy.2020.00104

[12] Ismail, G. M., Abdl-Rahim, H. R., Ahmad, H., & Chu, Y. M. Fractional residual power series method for the analytical and approximate studies of fractional physical phenomena, *Open Physics*, vol. 18, no 1, 2020, pp. 799-805. https://doi.org/10.1515/phys-2020-0190

[13] Eriqat, T., El-Ajou, A., Moa'ath, N. O., Al-Zhour, Z., & Momani, S. A new attractive analytic approach for solutions of linear and nonlinear neutral fractional pantograph equations, *Chaos, Solitons & Fractals*, vol. 138, 2020, pp. 109957. https://doi.org/10.1016/j.chaos.2020.109957

[14] Aljarrah, H., Alaroud, M., Ishak, A., & Darus, M. Approximate solution of nonlinear time-fractional PDEs by Laplace residual power series method, *Mathematics*, vol. 10, no 12, 2022, pp. 1980. https://doi.org/10.3390/math10121980

[15] Oqielat, M. A. N., Eriqat, T., Ogilat, O., El-Ajou, A., Alhazmi, S. E., & Al-Omari, S. Laplace-residual power series method for solving time-fractional reaction–diffusion model, *Fractal and Fractional*, vol. 7, no 4, 2023, pp. 309. https://doi.org/10.3390/fractalfract7040309

[16] Yadav, S., Vats, R. K., & Rao, A. Constructing the fractional series solutions for time-fractional K-dV equation using Laplace residual power series technique, *Optical and Quantum Electronics*, vol. 56, no 5, 2024, pp. 721. https://doi.org/10.1007/s11082-024-06412-9

[17] A. S. Hussain, K. D. Pati, A. K. Atiyah, and M. A. Tashtoush. Rate of occurrence estimation in geometric processes with Maxwell distribution: A comparative study between artificial intelligence and classical methods. *International Journal of Advances in Soft Computing and its Applications*, vol. 17, no 1, 2025, pp. 1-15. DOI: 10.15849/IJASCA.250330.01

[18] M. Berir. Analysis of the effect of white noise on the Halvorsen system of variable-order fractional derivatives using a novel numerical method. *International Journal of Advances in Soft Computing and its Applications*, vol. 16, no 3, 2024, pp. 294–306. DOI: 10.15849/IJASCA.241130.16

[19] P. Singh, N. Zade, P. Priyadarshi, and A. Gupte. The application of machine learning and deep learning techniques for global energy utilization projection for ecologically responsible energy management. *International Journal of Advances in Soft Computing and its Applications*, vol. 17, no 1, 2025, pp. 49–66. https://doi.org/10.15849/ijasca.250330.04

[20] H. Al-Taani, M. A. Hammad, O. Alomari, I. Bendib, and A. Ouannas. Finite-time control of the discrete Sel'kov–Schnakenberg model: Synchronization and simulations. *AIP Advances*, vol. 15, no 2, 2025, pp. 025325. https://doi.org/10.1063/5.0257304

[21] Ali, A., Shah, K., & Khan, R. A. Numerical treatment for traveling wave solutions of fractional Whitham-Broer-Kaup equations, Alexandria Eng. J, vol. 57, no 3, 2018, pp. 1991-1998. https://doi.org/10.1016/j.aej.2017.04.012

[22] Tenenbaum, M., & Pollard, H. Ordinary differential equations: an elementary textbook for students of mathematics, engineering, and the sciences, *Courier Corporation*, 1985.

[23] El-Ajou, A. Adapting the Laplace transform to create solitary solutions for the nonlinear time-fractional dispersive PDEs via a new approach, *The European Physical Journal Plus*, vol. 136, no 2, 2021, pp. 229. https://doi.org/10.1140/epjp/s13360-020-01061-9

Contribution of Individual Authors to the Creation of a Scientific Article (Ghostwriting Policy)

The authors equally contributed in the present research, at all stages from the formulation of the problem to the final findings and solution.

Sources of Funding for Research Presented in a Scientific Article or Scientific Article Itself

No funding was received for conducting this study.

Conflict of Interest

The authors have no conflicts of interest to declare that are relevant to the content of this article.

Appendix

Table 1: Absolute errors of the L-RPSM approximate solution $\mathfrak{u}(\zeta, \varrho)$ for different values of α ($\alpha = 1$, $\alpha = 0.75$, $\alpha = 0.5$ and $\alpha = 0.25$).

		Asolute errors				Exact. Sol
ϱ	ζ	$\alpha = 0.25$	$\alpha = 0.5$	$\alpha = 0.75$	$\alpha = 1$	$\alpha = 1$
2	2	5.85×10^{-5}	3.44×10^{-5}	1.44×10^{-5}	1.88×10^{-10}	-0.45974908
	4	3.68×10^{-5}	2.16×10^{-5}	9.08×10^{-6}	1.01×10^{-10}	-0.43255834
	6	2.48×10^{-5}	1.47×10^{-5}	5.83×10^{-6}	8.80×10^{-11}	-0.41528390
	8	1.54×10^{-5}	9.04×10^{-6}	3.80×10^{-6}	3.50×10^{-11}	-0.40410254
	10	1.01×10^{-5}	5.95×10^{-6}	2.50×10^{-6}	2.19×10^{-11}	-0.39677974
6	2	3.65×10^{-4}	2.76×10^{-4}	1.56×10^{-4}	5.09×10^{-9}	-0.46089068
	4	2.29×10^{-4}	1.91×10^{-4}	9.81×10^{-5}	2.72×10^{-9}	-0.43277291
	6	1.47×10^{-4}	1.11×10^{-4}	6.30×10^{-5}	1.57×10^{-9}	-0.41542089
	8	9.60×10^{-5}	7.27×10^{-5}	4.11×10^{-5}	9.47×10^{-10}	-0.40419240
	10	6.31×10^{-5}	4.78×10^{-5}	2.70×10^{-5}	5.91×10^{-10}	-0.39683887

”Source: created by the authors.”

Table 2: Absolute errors of the L-RPSM approximate solution $\mathfrak{v}(\zeta, \varrho)$ for different values of α ($\alpha = 1$, $\alpha = 0.75$, $\alpha = 0.5$ and $\alpha = 0.25$).

		Asolute errors				Exact. Sol
ϱ	ζ	$\alpha = 0.25$	$\alpha = 0.5$	$\alpha = 0.75$	$\alpha = 1$	Exact sol $\alpha = 1$
2	2	4.82×10^{-5}	2.83×10^{-5}	1.19×10^{-5}	2.17×10^{-10}	-0.058554331
	4	2.85×10^{-5}	1.68×10^{-5}	7.04×10^{-6}	1.01×10^{-10}	-0.036784994
	6	1.76×10^{-5}	1.03×10^{-5}	4.35×10^{-6}	5.23×10^{-11}	-0.023635701
	8	1.12×10^{-5}	6.56×10^{-6}	2.76×10^{-6}	2.92×10^{-11}	-0.015407833
	10	7.23×10^{-6}	4.24×10^{-6}	1.78×10^{-6}	1.72×10^{-11}	-0.010139120
6	2	3.01×10^{-4}	2.28×10^{-4}	1.29×10^{-4}	5.86×10^{-9}	-0.058831656
	4	1.78×10^{-4}	1.35×10^{-4}	7.62×10^{-5}	2.73×10^{-9}	-0.036951646
	6	1.10×10^{-4}	8.52×10^{-5}	4.78×10^{-5}	1.41×10^{-9}	-0.023733856
	8	6.97×10^{-5}	5.32×10^{-5}	2.93×10^{-5}	8.17×10^{-10}	-0.015473702
	10	4.50×10^{-5}	3.41×10^{-5}	1.93×10^{-5}	4.65×10^{-10}	-0.010181284

”Source: created by the authors.”

Table 3: Comparison of the L-RPSM with other existing methods for the approximate solution $\mathfrak{u}(\zeta, \varrho)$.

ϱ	ζ	**ADM, [7]**	**VIM, [8]**	**OHAM, [9]**	**B-spline, [10]**	**NIM(2), [11]**	**L-RPSM(2)**	**L-RPSM (3)**
0.1	0.1	1.05×10^{-4}	1.23×10^{-4}	1.07×10^{-4}	1.54×10^{-5}	1.67×10^{-12}	4.67×10^{-14}	1.11×10^{-16}
	0.3	9.64×10^{-5}	3.70×10^{-4}	3.05×10^{-4}	1.72×10^{-5}	4.51×10^{-11}	1.27×10^{-12}	1.11×10^{-16}
	0.5	8.88×10^{-5}	6.17×10^{-4}	4.81×10^{-4}	2.10×10^{-5}	2.09×10^{-10}	5.86×10^{-12}	1.33×10^{-15}
0.2	0.1	4.25×10^{-4}	1.20×10^{-4}	1.04×10^{-4}	1.61×10^{-5}	1.58×10^{-12}	4.51×10^{-14}	1.11×10^{-16}
	0.3	3.91×10^{-4}	3.60×10^{-4}	2.97×10^{-4}	1.94×10^{-5}	4.26×10^{-11}	1.22×10^{-12}	5.55×10^{-17}
	0.5	3.60×10^{-4}	6.01×10^{-4}	4.70×10^{-4}	2.64×10^{-5}	1.97×10^{-10}	5.63×10^{-12}	1.39×10^{-15}
0.3	0.1	9.72×10^{-4}	1.17×10^{-4}	1.02×10^{-4}	1.58×10^{-5}	1.49×10^{-12}	4.32×10^{-14}	1.11×10^{-16}
	0.3	8.93×10^{-4}	3.51×10^{-4}	2.90×10^{-4}	1.92×10^{-5}	4.03×10^{-11}	1.17×10^{-12}	1.67×10^{-16}
	0.5	8.22×10^{-4}	5.86×10^{-4}	4.60×10^{-4}	2.62×10^{-5}	1.86×10^{-10}	5.42×10^{-12}	1.17×10^{-15}
0.4	0.1	1.76×10^{-3}	1.14×10^{-4}	9.92×10^{-5}	1.44×10^{-5}	1.41×10^{-12}	4.17×10^{-14}	5.55×10^{-17}
	0.3	1.61×10^{-3}	3.42×10^{-4}	2.83×10^{-4}	1.63×10^{-5}	3.81×10^{-11}	1.13×10^{-12}	1.67×10^{-16}
	0.5	1.49×10^{-3}	5.71×10^{-4}	4.49×10^{-4}	2.02×10^{-5}	1.76×10^{-10}	5.21×10^{-12}	1.28×10^{-15}
0.5	0.1	2.80×10^{-3}	1.11×10^{-4}	9.68×10^{-4}	1.23×10^{-5}	1.33×10^{-12}	4.00×10^{-14}	1.11×10^{-16}
	0.3	2.57×10^{-3}	3.33×10^{-4}	2.76×10^{-4}	1.23×10^{-5}	3.60×10^{-11}	1.08×10^{-12}	1.11×10^{-16}
	0.5	2.36×10^{-3}	5.56×10^{-4}	4.39×10^{-4}	1.23×10^{-5}	1.67×10^{-10}	5.02×10^{-12}	1.11×10^{-15}

”Source: created by the authors.”

Table 4: Comparison of the L-RPSM with other existing methods for the approximate solution $\mathfrak{v}(\zeta, \varrho)$.

ϱ	ζ	**ADM, [7]**	**VIM, [8]**	**OHAM, [9]**	**B-spline, [10]**	**NIM(2), [11]**	**L-RPSM(2)**	**L-RPSM (3)**
0.1	0.1	6.41×10^{-3}	1.10×10^{-4}	5.87×10^{-5}	3.11×10^{-5}	3.28×10^{-12}	6.37×10^{-14}	1.39×10^{-17}
	0.3	5.99×10^{-3}	3.32×10^{-4}	3.05×10^{-4}	4.80×10^{-5}	8.86×10^{-11}	1.72×10^{-12}	3.33×10^{-16}
	0.5	5.62×10^{-3}	5.54×10^{-4}	3.09×10^{-4}	8.20×10^{-5}	4.10×10^{-10}	7.96×10^{-12}	2.41×10^{-15}
0.2	0.1	1.33×10^{-2}	1.07×10^{-4}	5.57×10^{-5}	1.53×10^{-5}	3.08×10^{-12}	6.07×10^{-14}	5.55×10^{-17}
	0.3	1.24×10^{-2}	3.22×10^{-4}	2.97×10^{-4}	2.29×10^{-5}	8.31×10^{-11}	1.64×10^{-12}	3.33×10^{-16}
	0.5	1.16×10^{-2}	5.37×10^{-4}	2.93×10^{-4}	3.50×10^{-5}	3.85×10^{-10}	7.58×10^{-12}	2.32×10^{-15}
0.3	0.1	2.08×10^{-2}	1.04×10^{-4}	5.29×10^{-5}	3.37×10^{-7}	2.89×10^{-12}	5.77×10^{-14}	1.39×10^{-17}
	0.3	1.94×10^{-2}	3.12×10^{-4}	2.90×10^{-4}	3.59×10^{-6}	7.80×10^{-11}	1.56×10^{-12}	2.91×10^{-16}
	0.5	1.81×10^{-2}	5.20×10^{-4}	2.77×10^{-4}	1.66×10^{-5}	3.61×10^{-10}	7.22×10^{-12}	2.15×10^{-15}
0.4	0.1	2.88×10^{-2}	1.01×10^{-4}	5.02×10^{-5}	1.41×10^{-5}	2.71×10^{-12}	5.51×10^{-14}	2.78×10^{-17}
	0.3	2.69×10^{-2}	3.02×10^{-4}	2.83×10^{-4}	2.87×10^{-5}	7.32×10^{-11}	1.49×10^{-12}	2.36×10^{-16}
	0.5	2.51×10^{-2}	5.05×10^{-4}	2.63×10^{-4}	6.51×10^{-5}	3.39×10^{-10}	6.88×10^{-12}	2.04×10^{-15}
0.5	0.1	3.75×10^{-2}	9.75×10^{-5}	4.77×10^{-5}	1.08×10^{-5}	2.55×10^{-12}	5.25×10^{-14}	2.78×10^{-17}
	0.3	3.50×10^{-2}	2.93×10^{-4}	2.76×10^{-4}	1.08×10^{-5}	6.88×10^{-11}	1.42×10^{-12}	2.78×10^{-16}
	0.5	3.26×10^{-2}	4.89×10^{-4}	2.49×10^{-4}	1.08×10^{-5}	3.19×10^{-10}	6.56×10^{-12}	1.92×10^{-15}

”Source: created by the authors.”